

Supplementary Information for

**Experimental Identification of Aminomethanol  
(NH<sub>2</sub>CH<sub>2</sub>OH) – The Key Intermediate in the Strecker  
Synthesis**

Santosh K. Singh<sup>1</sup>, Cheng Zhu<sup>1</sup>, Jesse La Jeunesse<sup>1</sup>, Ryan C. Fortenberry<sup>2\*</sup>, Ralf I. Kaiser<sup>1\*</sup>

<sup>1</sup>*Department of Chemistry, University of Hawaii, 2545 McCarthy Mall, Honolulu, HI 96822, USA.*

*W. M. Keck Research Laboratory in Astrochemistry, University of Hawaii, 2545 McCarthy Mall, Honolulu, HI 96822, USA.*

<sup>2</sup>*Department of Chemistry and Biochemistry, University of Mississippi, 322 Coulter Hall, University, MS 38677-1848, USA.*

Correspondence to: [ralfk@hawaii.edu](mailto:ralfk@hawaii.edu), [r410@olemiss.edu](mailto:r410@olemiss.edu)

**This PDF file includes:**

Supplementary Methods  
Supplementary Figures 1 to 5  
Supplementary Tables 1 to 5  
Supplementary References

## Supplementary Methods

1. Calculations of column densities of methylamine ( $\text{CH}_3\text{NH}_2$ ) and oxygen ( $\text{O}_2$ ) in the ice mixture.

The column density of methylamine ( $N_{\text{CH}_3\text{NH}_2}$ ) in the ice mixture was determined to be  $5.3 \pm 0.5 \times 10^{16}$  molecules  $\text{cm}^{-2}$  using the integrated area of the IR absorption band  $\nu_3$  ( $2794 \text{ cm}^{-1}$ ) of methylamine and its corresponding integral absorption coefficient ( $A_{\text{exp}}$ ) of  $1.0 \times 10^{-18} \text{ cm molecule}^{-1}$  in equation 1;<sup>1</sup>

$$N_{\text{CH}_3\text{NH}_2} = \frac{\ln 10 \int_{\nu_1}^{\nu_2} A_\nu d\nu \cos(\theta)}{A_{\text{exp}} 2} \quad (1)$$

where  $\int_{\nu_1}^{\nu_2} A_\nu d\nu$  is the integrated peak area of the absorbance in the region  $\nu_1$ - $\nu_2 \text{ cm}^{-1}$ ,  $A_{\text{exp}}$  is the integrated absorption coefficient and  $\theta$  is the angle of incidence ( $45^\circ$ ) of the IR beam. On the other hand, the column density of the oxygen molecule cannot be directly determined from the FTIR spectrum because its vibrational mode is IR inactive. To determine the column density of  $\text{O}_2$ , we first calculated the thickness of methylamine ( $\text{CH}_3\text{NH}_2$ ) in the ice mixture ( $\text{CH}_3\text{NH}_2 + \text{O}_2$ ) using equation 2

$$d_{\text{CH}_3\text{NH}_2} = \frac{\ln 10 M \int_{\nu_1}^{\nu_2} A_\nu d\nu}{2N_A \rho n A_{\text{exp}}} \sqrt{n^2 - \sin^2 \theta} \quad (2)$$

where  $M$  is the molecular weight,  $N_A$  is the Avogadro's number,  $\rho$  is the density of methylamine ice ( $0.85 \text{ g cm}^{-3}$ )<sup>1</sup> and  $n$  is the refractive index of methylamine ( $n = 1.40$ )<sup>1</sup>. From equation 2, the thickness of methylamine ice in the ice mixture was determined to be  $39 \pm 4 \text{ nm}$ . The total thickness of the ice mixture ( $d_t = 239 \pm 24 \text{ nm}$ ) was determined using equation 3.

$$d_t = \frac{m\lambda}{2\sqrt{n^2 - \sin^2 \varphi}} \quad (3)$$

Where,  $m$  is the number of interference fringes ( $m=1$ ) observed after reflection of the He-Ne laser light ( $\lambda = 632.8 \text{ nm}$ ) from the silver substrate and ice surface,  $\varphi$  ( $=4^\circ$ ) is the incidence angle of the laser, and  $n$  is the average refractive index. Next, we determined the  $\text{O}_2$  ice thickness ( $d_{\text{O}_2}$ ) to be  $200 \pm 20 \text{ nm}$ , by subtracting the methylamine ice thickness ( $d_{\text{CH}_3\text{NH}_2}$ ) from the total thickness ( $d_t$ ) of the ice mixture (equation 4).

$$d_{\text{O}_2} = d_t - d_{\text{CH}_3\text{NH}_2} \quad (4)$$

$$N_{\text{O}_2} = \frac{d_{\text{O}_2} 2N_A \rho n}{M \sqrt{n^2 - \sin^2 \theta}} \frac{\cos(45^\circ)}{2} \quad (5)$$

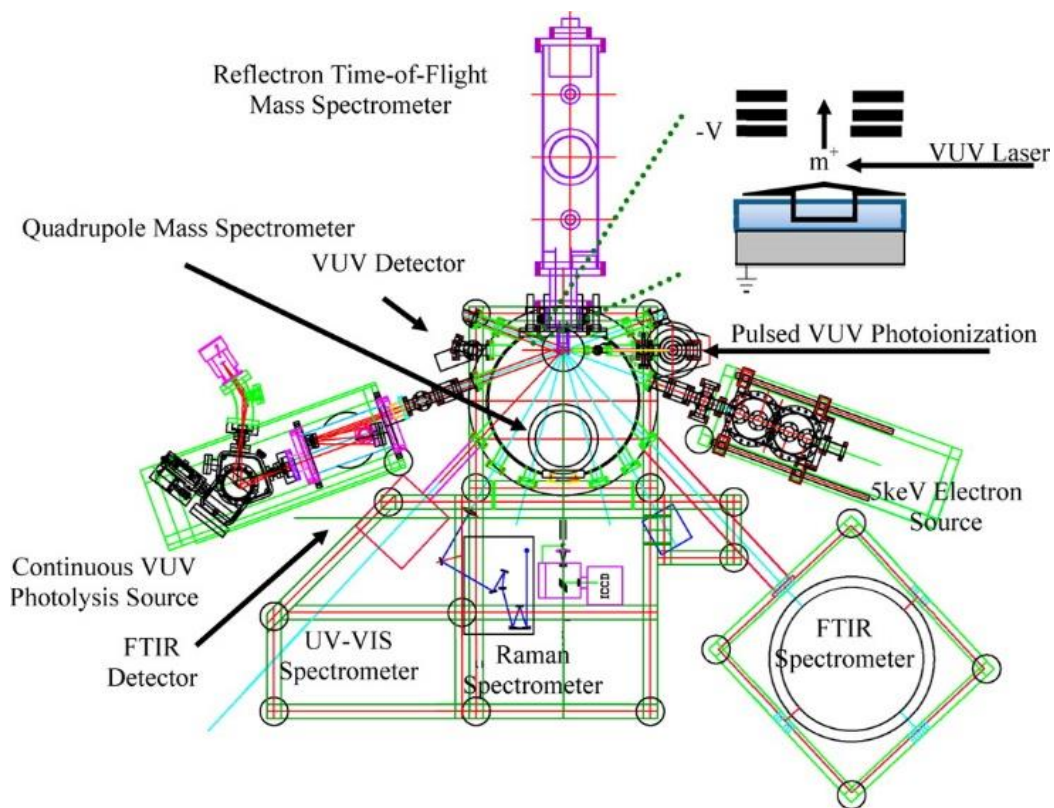
Using thickness ( $d_{O_2} = 200 \text{ nm}$ ), density ( $\rho = 1.54 \text{ g cm}^{-3}$ ) and refractive index ( $n = 1.25$ )<sup>2</sup> of  $O_2$  ice in eq. 5, the column density of the oxygen in the ice mixture is determined to be  $49 \pm 5 \times 10^{16} \text{ molecules cm}^{-2}$ .

## 2. Generation of VUV light

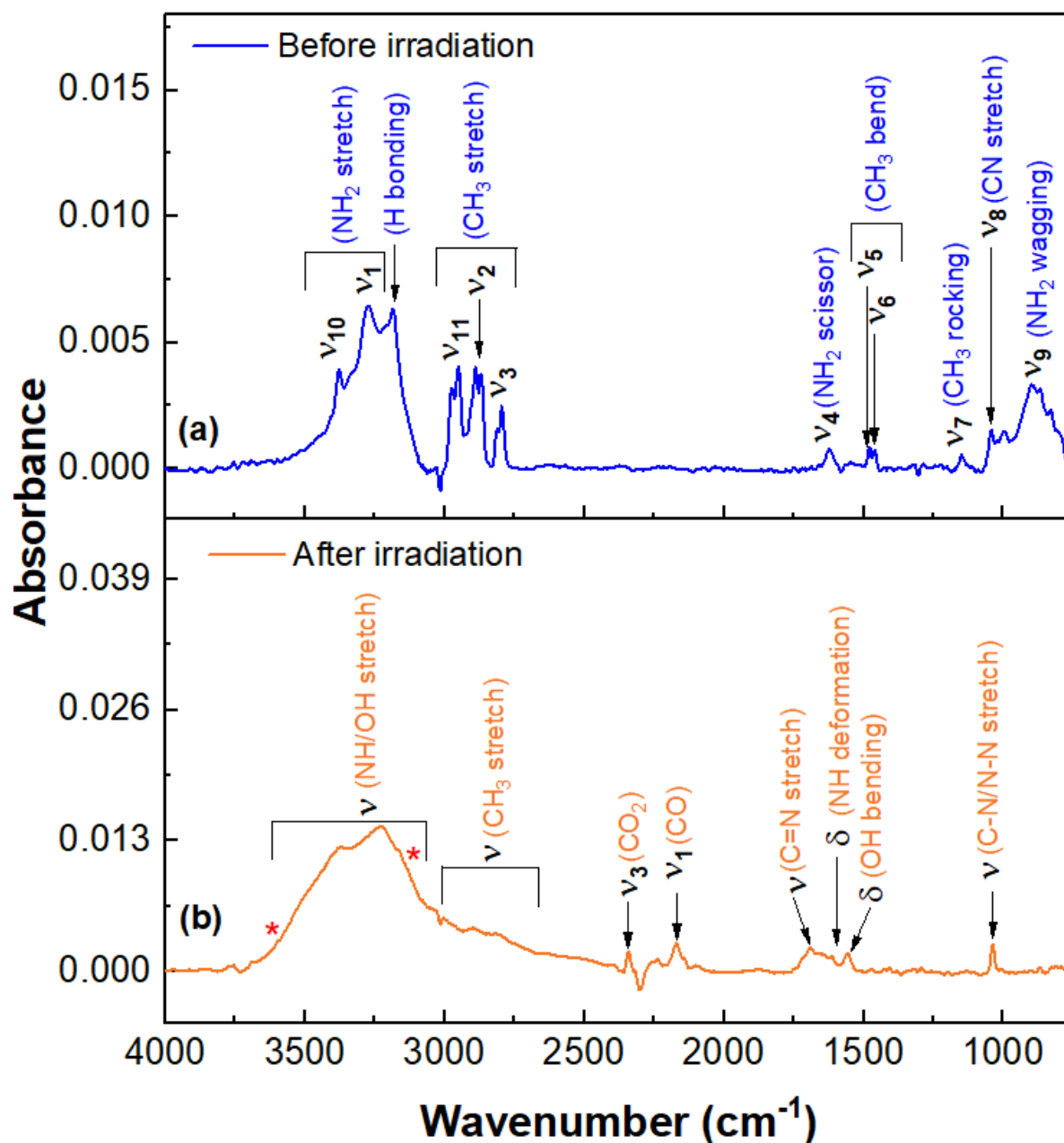
(I) 9.50 eV – The second harmonics (532 nm) of a pulsed ND:YAG laser (Spectra Physics, PRO-250-30; 30 Hz, 10 ns) was used to pump a dye laser (Sirah Cobra Stretch) having Rhodamine 610/640 dye mixture. The fundamental output of the dye laser (606.948 nm) undergoes frequency tripling to generate 202.316 nm ( $\omega_1$ ) light. Two photons of  $\omega_1$  is required to access the resonant transition of Krypton. The third harmonics (355 nm) of a second ND:YAG laser (Spectra Physics, PRO-250-30; 30 Hz, 10 ns) was used to pump another dye laser (Sirah Cobra Stretch) containing Coumarin 450 dye to generate 449.794 nm ( $\omega_2$ ) light. The 202 nm and 449.794 nm lights were spatially and temporally overlapped on pulsed jet of Krypton (80  $\mu\text{s}$ , 30 Hz) which act as a non-linear medium. Difference frequency mixing of two photons of  $\omega_1$  and one photon of  $\omega_2$  in Krypton ( $2\omega_1 - \omega_2$ ) results in the generation of 130.51 nm ( $\omega_{\text{VUV}} = 9.50 \text{ eV}$ ) light. A LiF biconvex lens is used to separate the 130.51 nm light from residual 202 nm and 449.794 nm lights.

(II) 9.10 eV – The 136.24 nm (9.10 eV) light was generated via difference frequency mixing of two photons of 222.566 nm ( $\omega_1$ ) and one photon of 579.014 nm ( $\omega_2$ ) light in xenon. To produce  $\omega_1$ , the fundamental output of a dye laser (445.132, Coumarin 450), pumped by the third harmonics (355 nm) of an ND:YAG laser (Spectra Physics, PRO-250-30; 30 Hz, 10 ns), was frequency doubled through a BBO crystal. The second harmonics (532 nm) of a pulsed ND:YAG laser was used to pump another dye laser having Pyrromethane 593 dye to generate  $\omega_2$  (579.014 nm). The  $\omega_1$  and  $\omega_2$  lights were spatially and temporally overlapped on the pulsed jet of Krypton for difference frequency generation of 136.24 nm light. The generated VUV light (136.24 nm) is eventually separated from the residual 222.566 nm and 579.014 nm lights by the help of a LiF biconvex lens and directed at about 2 mm above the sample to ionize the subliming molecules.

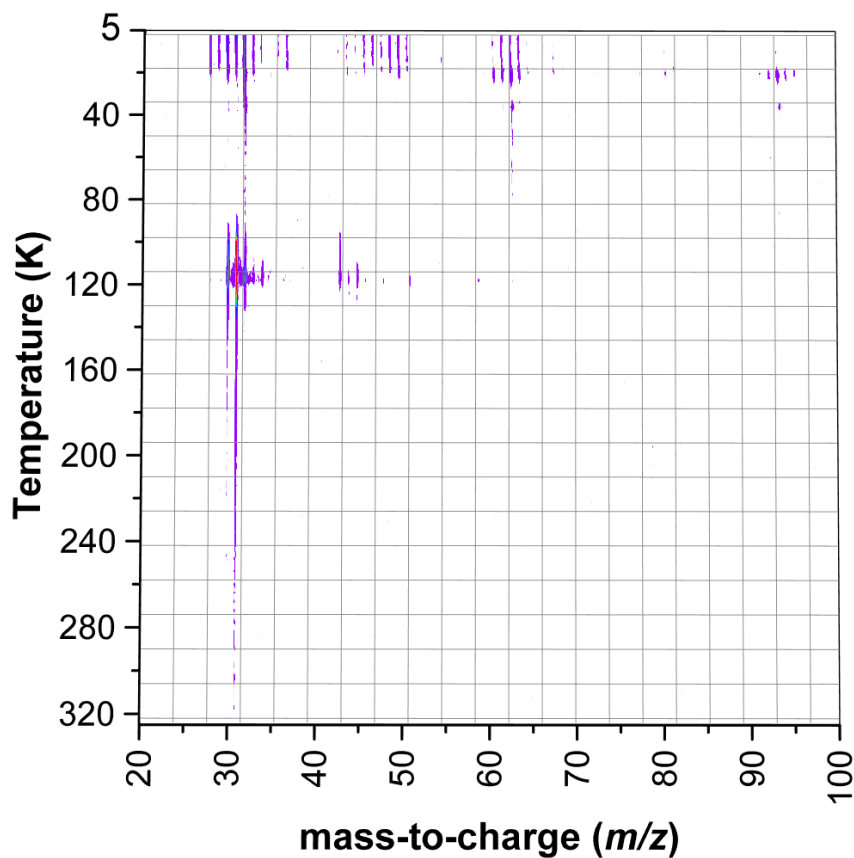
## Supplementary Figures



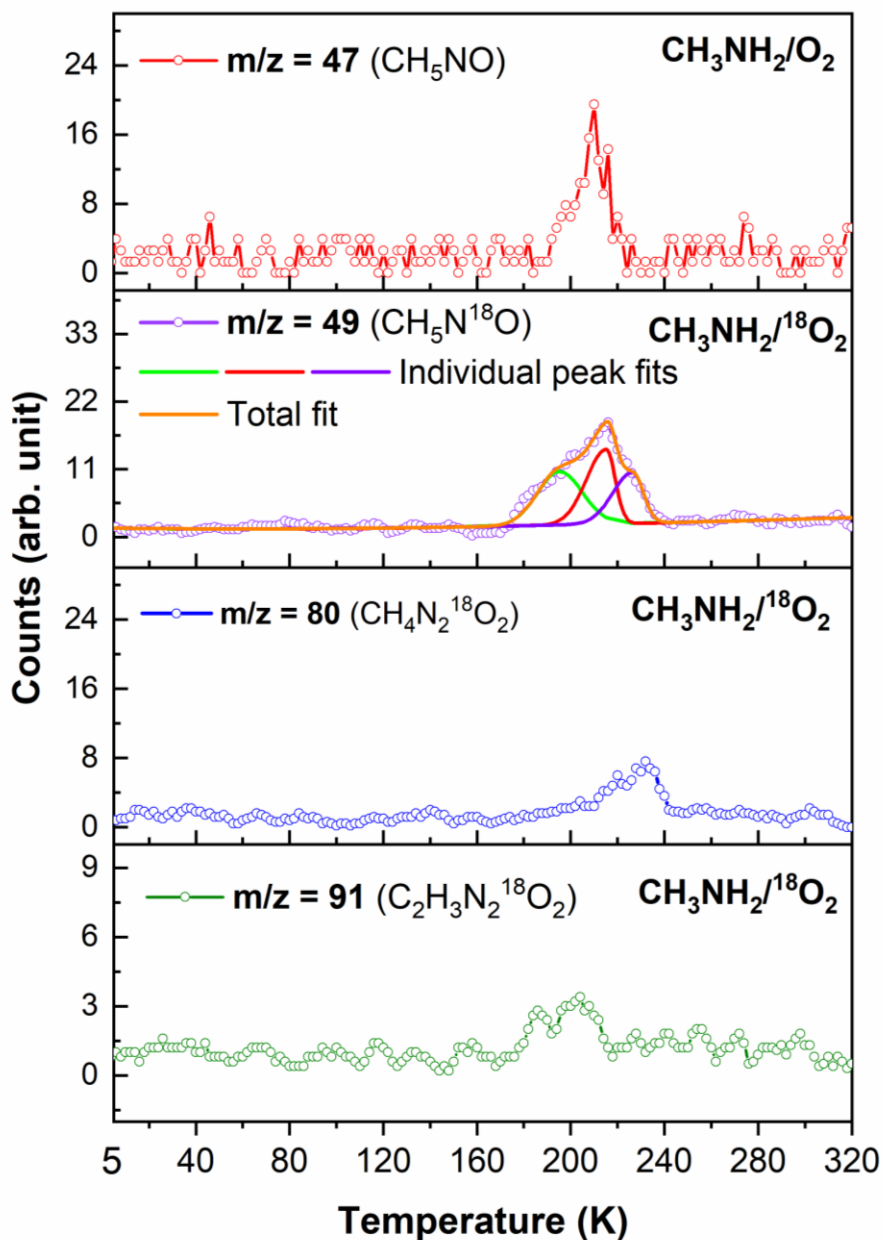
**Supplementary Figure 1.** Schematic top view of the ultra-high vacuum chamber including the electron source, analytical instruments (FTIR, UV-VIS, ReTOF), and cryogenic target (point of convergence lines).<sup>3,4</sup> Adapted with permission from ref. 3. Copyright (2013) American Chemical Society.



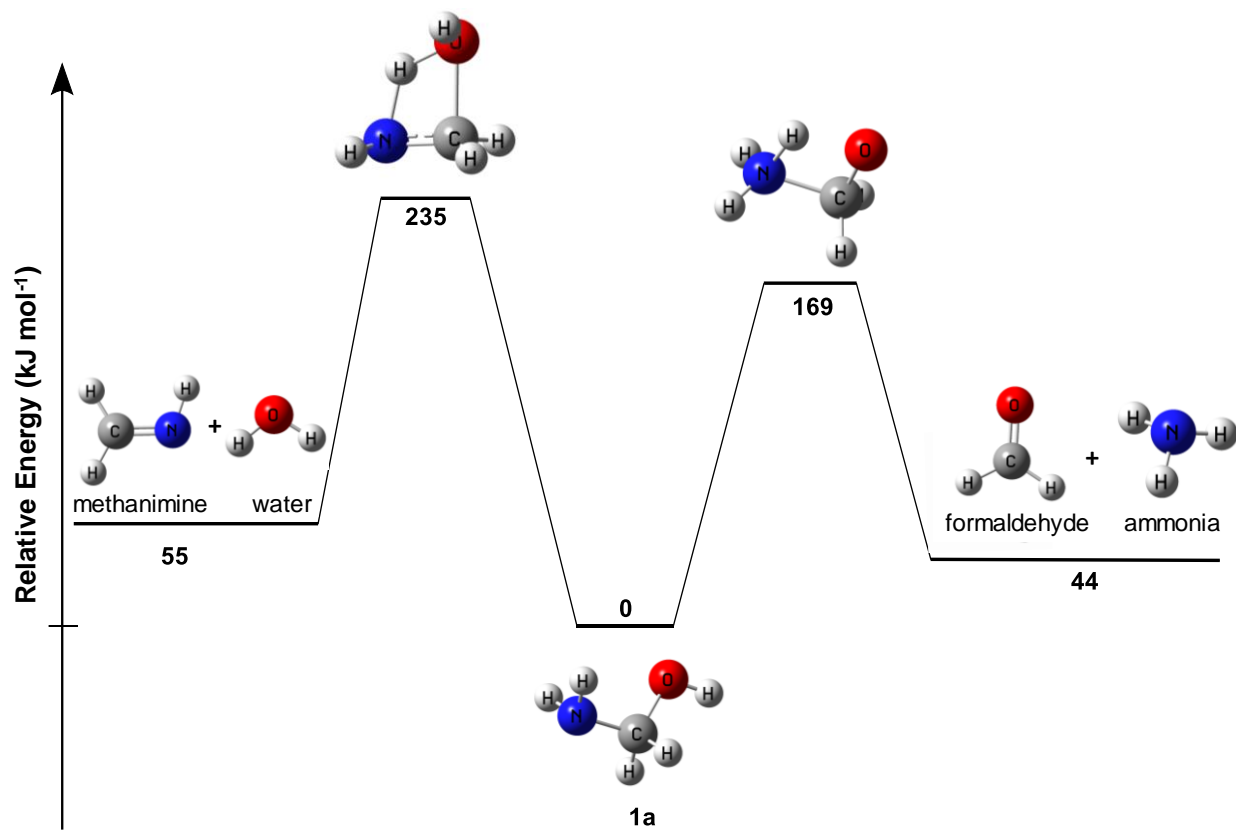
**Supplementary Figure 2.** Infrared spectra of methylamine and oxygen ice mixture (a) before and (b) after irradiation at 5 K. Vibrational modes of methylamine ( $\nu_1 - \nu_{11}$ ) are labeled in (a). New absorption bands observed after irradiation are labeled in (b). The calculated and scaled -OH ( $3659 \text{ cm}^{-1}$ ) and -NH<sub>2</sub> ( $3146 \text{ cm}^{-1}$ ) stretching vibrations of aminomethanol (**1**) are marked with asterisks. Scaling factors of 0.96 and 0.95 were used to scale the calculated -OH and -NH<sub>2</sub> stretches of **1**, respectively. These scaling factors were determined by dividing experimental -OH ( $3656 \text{ cm}^{-1}$ ) and -NH<sub>2</sub> ( $3312 \text{ cm}^{-1}$ ) vibrational frequencies of N-methylhydroxylamine<sup>5</sup> (**4**) by corresponding calculated frequencies. The unscaled vibrational frequencies of aminomethanol isomers are provided in Supplementary Data 2. Source data are provided as a Source Data file.



**Supplementary Figure 3.** PI-ReTOF mass spectrum measured as a function of temperature during the TPD phase of non-irradiated methylamine ( $\text{CH}_3\text{NH}_2$ ) and oxygen ( $\text{O}_2$ ) ice mixture at a photon energy of 10.49 eV. The dark colored purple lines indicate ion counts. Source data are provided as a Source Data file.



**Supplementary Figure 4.** PI-ReTOF mass spectra measured at  $m/z = 49$ , 80 and 91 during the sublimation phase of irradiated  $\text{CH}_3\text{NH}_2 - ^{18}\text{O}_2$  ice mixture along with the mass spectrum recorded at  $m/z = 47$  in non-isotopic system ( $\text{CH}_3\text{NH}_2 - \text{O}_2$ ) at a photon energy of 9.50 eV. Source data are provided as a Source Data file.



**Supplementary Figure 5.** Decomposition pathways of aminomethanol calculated at the CCSD(T)/CBS//MP2/aug-cc-pVTZ level of theory. Coordinates of the transition states are provided in Supplementary Table 5.

## Supplementary Tables

**Supplementary Table 1.** Data applied to calculate the average dose per molecule.

---

Initial Kinetic energy of the electrons	5 keV
Irradiation current (I)	$100 \pm 10$ nA
Irradiation time (t)	3600 s
Average penetration depth, l	$202 \pm 20$ nm
Average kinetic energy of backscattered electrons, $E_{bs}^a$	$3.3 \pm 0.3$ keV
Fraction of backscattered electrons, $f_{bs}^a$	$0.35 \pm 0.04$
Average kinetic energy of transmitted electrons, $E_{trans}^a$ ,	0.0 keV
Fraction of transmitted electrons, $f_{trans}^a$	0
Average density of the ice mixture, $\rho$	$1.20$ g cm <sup>-3</sup>
Irradiated area, A	$1.0 \pm 0.2$ cm <sup>2</sup>
total number of molecules processed	$4.5 \pm 0.5 \times 10^{17}$
dose per molecule, D	methylamine: $18.3 \pm 0.2$ eV oxygen: $18.9 \pm 2.3$ eV
Total number of electrons	$2.2 \pm 0.2 \times 10^{15}$

---

<sup>a</sup> Values from CASINO simulations.

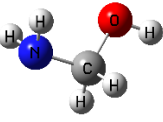
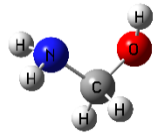
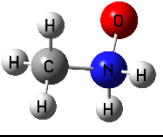
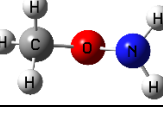
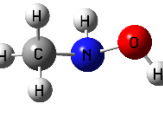
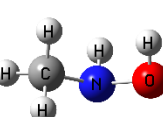
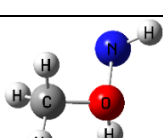
**Supplementary Table 2.** (a) Infrared features of methylamine-oxygen ice mixture before irradiation and (b) new vibrational bands appeared after irradiation at 5 K.

(a) Before Irradiation				
wavenumber observed (cm <sup>-1</sup> )	wavenumber literature (cm <sup>-1</sup> ) <sup>1</sup>	assignments	carrier	Ref.
3376	3332	$\nu_{10}$	NH <sub>2</sub> asymm. stretch	(1)
3274	3260	$\nu_1$	NH <sub>2</sub> symm. stretch	(1)
3185	3191		H-bonding	(1)
2950	2942	$\nu_{11}$	CH <sub>3</sub> stretch	(1)
2886	2881	$\nu_2$	CH <sub>3</sub> stretch	(1)
2794	2793	$\nu_3$	CH <sub>3</sub> symm. stretch	(1)
1623	1651	$\nu_4$	NH <sub>2</sub> scissor	(1)
1479	1467	$\nu_5$	CH <sub>3</sub> deformation	(1)
1459	1441	$\nu_6$	CH <sub>3</sub> deformation	(1)
1149	1182	$\nu_7$	CH <sub>3</sub> rocking	(1)
1043	1048	$\nu_8$	C-N stretch	(1)
900	955	$\nu_9$	NH <sub>2</sub> wagging	(1)
(b) After Irradiation				
3680-3000	3700-3000	$\nu$ (-OH/-NH-)	O-H/N-H stretch	(6)
3000-2800	3000-2800	$\nu$ (-CH <sub>3</sub> /-CH <sub>2</sub> -)	C-H stretch	(6)
2343	2343	$\nu_3$ (CO <sub>2</sub> )	C=O stretch	(7)
2169	2137	$\nu_1$ (CO)	C≡O stretch	(7)
1693	1662	$\nu$ (-C=N-)	C=N stretch	(8)
1612	1616	$\delta$ (-NH-)	N-H deformation	(9)
1556		$\delta$ (-OH)	O-H bending	
1039		$\nu$ (C-N/N-N)	C-N/N-N stretch	

**Supplementary Table 3.** Parameters for the vacuum ultraviolet (VUV) light generated in the present study

<b>Photon energy (eV)</b>		<b>9.50</b>	<b>9.10</b>
Nd:YAG ( $\omega_1$ )	Wavelength (nm)	532	355
Dye laser ( $\omega_1$ )	Wavelength (nm)	606.948	445.132
Dye		Rh 610/ Rh 640	Coumarin 450
$\omega_2$	Wavelength (nm)	449.794	579.014
Nd:YAG ( $\omega_2$ )	Wavelength (nm)	355	532
Dye laser ( $\omega_2$ )	Wavelength (nm)	449.794	579.014
Dye		Coumarin 450	Pyrrromethane 593
	Nonlinear medium	Kr	Xe

**Supplementary Table 4.** Calculated adiabatic ionization energies (IE) and relative energies ( $E_{\text{rel}}$ ) of distinct  $\text{CH}_5\text{ON}$  isomers. Values calculated at the CCSD(T)/CBS//CCSD(T)/aug-cc-pVTZ level of theory (blue color text) are considered for comparison with the experiment

Structure	Name	DFT/CCSD(T)		CCSD(T)		
		IE (eV) <sup>a</sup>	$E_{\text{rel}}$ (kJ mol <sup>-1</sup> ) <sup>b</sup>	IE (eV) <sup>c</sup>	IE range (eV) <sup>d</sup>	$E_{\text{rel}}$ (kJ mol <sup>-1</sup> ) <sup>e</sup>
	$C_s$ -aminomethanol <b>(1a)</b>	9.39	0.00	9.28	9.30 – 9.23	0
	$C_1$ -aminomethanol <b>(1b)</b>	9.41	2.28	9.30	9.32 – 9.25	2
	methanamine oxide <b>(2)</b>	8.97	243.05	8.82	8.84 – 8.77	239
	O-methylhydroxylamine <b>(3)</b>	8.74	181.28	8.70	8.72 – 8.65	173
	<i>E</i> -N-methylhydroxylamine <b>(4a)</b>	8.63	156.63	8.55	8.57 – 8.50	151
	<i>Z</i> -N-methylhydroxylamine <b>(4b)</b>	8.49	169.79	8.41	8.43 – 8.36	165
	(methyloxonio)amide <b>(5)</b>	7.69	434.24	7.58	7.60 – 7.53	420

<sup>a</sup> Adiabatic ionization potential by CCSD(T)/CBS with B3LYP/aug-cc-pVTZ ZPVE correction in eV.

<sup>b</sup> Relative energy by CCSD(T)/CBS with B3LYP/aug-cc-pVTZ ZPVE correction in kJ mol<sup>-1</sup>.

<sup>c</sup> Adiabatic ionization potential by CCSD(T)/CBS from the CCSD(T)/aug-cc-pVTZ geometry and with ZPVE correction in eV.

<sup>d</sup> IE range is determined by including the error limits (-0.05 to +0.02 eV) from ref. 10 in the calculated (CCSD(T)/CBS//CCSD(T)/aug-cc-pVTZ) IE values and subtracting 0.03 eV to correct for the electric field effect.

<sup>e</sup> Relative energy by CCSD(T)/CBS from the CCSD(T)/aug-cc-pVTZ geometry with ZPVE correction in kJ mol<sup>-1</sup>.

**Supplementary Table 5.** Coordinates of the transition states depicted in Supplementary Figure 5

TS (1a →formaldehyde + ammonia)			
	X	Y	Z
C	-0.258986	0.615775	0.000000
O	-1.108789	-0.428744	0.000000
H	0.206646	-1.007593	0.000000
H	-0.244251	1.249930	-0.898680
H	-0.244251	1.249930	0.898680
N	1.063102	-0.211535	0.000000
H	1.631315	-0.140041	0.838061
H	1.631315	-0.140041	-0.838061

TS (1a →methanimine + water)			
	X	Y	Z
C	-0.086560	-0.097928	-0.103223
O	0.025315	0.088776	1.674187
H	1.064594	-0.217021	1.094081
H	0.082160	1.036320	1.877013
H	-0.581014	0.800034	-0.471556
H	-0.724120	-0.971654	-0.044800
N	1.241594	-0.313321	-0.249228
H	1.702148	0.546533	-0.536568

## Supplementary References

1. Frigge, R. *et al.* A vacuum ultraviolet photoionization study on the formation of N-methyl formamide (HCONHCH<sub>3</sub>) in deep space: A potential interstellar molecule with a peptide bond. *Astrophys. J.* **862**, 84, (2018).
2. Jones, B. M., Kaiser, R. I. & Strazzulla, G. UV-VIS, infrared, and mass spectroscopy of electron irradiated frozen oxygen and carbon dioxide mixtures with water. *Astrophys. J.* **781**, 85, (2014).
3. Jones, B. M. & Kaiser, R. I. Application of reflectron time-of-flight mass spectroscopy in the analysis of astrophysically relevant ices exposed to ionization radiation: Methane (CH<sub>4</sub>) and D<sub>4</sub>-methane (CD<sub>4</sub>) as a case study. *J. Phys. Chem. Lett.* **4**, 1965-1971, (2013).
4. Bennett, C. J. *et al.* High-sensitivity Raman spectrometer to study pristine and irradiated interstellar ice analogs. *Analytical Chemistry* **85**, 5659-5665, (2013).
5. Davies, M. & Spiers, N. A. in *Adv. Molecular Spectrosc.* (ed A. Mangini) 761 (Pergamon, 1962)
6. Socrates, G. Infrared and Raman characteristic group frequencies. Tables and charts, John Wiley and Sons, Ltd, Chichester, Third Edition, 2001.
7. Zhu, C., Turner, A. M., Abplanalp, M. J. & Kaiser, R. I. Formation and high-order carboxylic Acids (RCOOH) in interstellar analogous ices of carbon dioxide (CO<sub>2</sub>) and methane (CH<sub>4</sub>). *Astrophys. J. Suppl. Ser.* **234**, 15, (2018).
8. Zhu, C. *et al.* A vacuum ultraviolet photoionization study on the formation of methanimine (CH<sub>2</sub>NH) and ethylenediamine (NH<sub>2</sub>CH<sub>2</sub>CH<sub>2</sub>NH<sub>2</sub>) in low temperature interstellar model ices exposed to ionizing radiation. *Phys. Chem. Chem. Phys.* **21**, 1952-1962, (2019).
9. Zheng, W. & Kaiser, R. I. Formation of hydroxylamine (NH<sub>2</sub>OH) in electron-irradiated ammonia–water ices. *J. Phys. Chem. A* **114**, 5251-5255, (2010).
10. Turner, A. M., Chandra, S., Fortenberry, R. C. & Kaiser, R. I. A Photoionization reflectron time-of-flight mass spectrometric study on the detection of ethynamine (HCCNH<sub>2</sub>) and 2H-Azirine (c-H<sub>2</sub>CCHN). *ChemPhysChem* **22**, 985-994, (2021).